

## Radiation generation by photoswitched, periodically biased semiconductors

E. Esarey, P. Sprangle, B. Hafizi,<sup>\*</sup> and P. Serafim<sup>†</sup>

*Beam Physics Branch, Plasma Physics Division, Naval Research Laboratory, Washington, D.C. 20375-5346*

(Received 29 September 1995)

A laser pulse, propagating nearly parallel to the surface of a planar semiconductor wafer, will generate electron-hole pairs. If the semiconductor is spatially biased with a static electric field of period  $\lambda_0$ , the laser pulse acts as a fast switch and generates a periodic current. The rapid switching of the current generates radiation, which propagates along the surface and can be confined by a conducting wall placed parallel to the wafer. The wavelength of the radiation can be tuned by adjusting  $\lambda_0$ , the wafer-wall separation, and/or the carrier density. In the absence of collisional damping,  $N_0$  periods of the static bias electric field will generate  $N_0$  periods of radiation. Under idealized conditions, the maximum electric field of the radiation is equal to the applied static field and the maximum efficiency of converting the static electric field energy to electromagnetic energy is 30%. In practice for typical parameters, tunable electromagnetic radiation can be generated with wavelengths in the 50–500- $\mu\text{m}$  range, pulse durations in the picosecond or subpicosecond range, and peak powers on the order of 100 W.

PACS number(s): 41.60.-m, 42.55.Px, 42.72.Ai

### I. INTRODUCTION

Over the past few years, several methods for the generation of picosecond and subpicosecond far-infrared radiation by optical switching of biased semiconductors have been investigated [1–10]. Most of these investigations have involved a planar photoconductor (typically, GaAs or InP) which is illuminated by ultrashort laser pulses. When the semiconductor is biased with a uniform static electric field, the photoswitching of the semiconductor produces a current transient which results in the generation of a single cycle of coherent radiation. For example, You *et al.* [7] report the generation of high power ( $\sim\text{MW}$ ) half-cycle pulses with durations  $<0.5$  ps and energies  $<0.8$   $\mu\text{J}$ . This was achieved by illuminating a  $3.5\times 3.5\text{-cm}^2$  GaAs wafer, biased with an external field of 11 kV/cm, with a 120-fs pulse from a Ti:sapphire laser at normal incidence.

Other photoconductor-based schemes have been investigated for generating many cycles of far-infrared radiation. For example, Froberg *et al.* [5] used a photoconducting antenna array to produce terahertz radiation pulses. This array was formed by depositing 64 electrodes, of width 20  $\mu\text{m}$  and spaced 150  $\mu\text{m}$  apart, on a GaAs substrate. The electrodes were then used to bias the photoconductor with a periodic electric field of wavelength  $\lambda_0$ . When illuminated with laser pulses incident on the substrate at an angle of  $\phi$  from the normal, radiation was produced over a wide range of angles, and the wavelength of the radiation at an angle  $\theta$  from normal was found to be  $\lambda \approx (\sin\theta + \sin\phi)\lambda_0$ . The frequency of the radiation could be adjusted by changing the angles  $\phi$  and  $\theta$ , and/or the biasing period  $\lambda_0$ . This method was used to produce low power ( $\sim\text{nW}$ ) 500-GHz radiation in 20-ps pulses.

Recently, an alternative concept for generating far-infrared radiation was proposed by Mori *et al.* [11], which relies on the conversion of a periodic static electric field into radiation by a relativistic ionization front. In this device, a parallel plate capacitor array is used to generate a periodic electric field within a gas. An intense, short laser pulse is injected into the gas, propagating parallel to the capacitor plates. As the laser pulse propagates, it ionizes the gas and produces free plasma electrons (photocarriers). A current transient is generated along the relativistic ionization front, resulting in the generation of electromagnetic radiation which propagates in either the direction of or opposite to the laser pulse. In the one-dimensional (1D) limit, and in the limit where the ionization front is moving at the speed of light in vacuum  $c$ , radiation is generated with frequency  $\omega$  given by  $\omega/c = (k_0^2 + k_p^2)/2k_0$ , where  $k_0 = 2\pi/\lambda_0$ ,  $\lambda_0$  is the period of the static electric field,  $k_p = \omega_p/c$ ,  $\omega_p = (4\pi n_e e^2/m_e)^{1/2}$  is the electron plasma frequency, and  $n_e$  is the density of the plasma electrons. Furthermore, the number of cycles of output radiation is roughly equal to the number of periods of the static electric field. Hence the frequency of the radiation can be tuned by adjusting the static field wavelength  $\lambda_0$  and/or the electron plasma density  $n_e$ . Furthermore, the output pulse duration can be controlled by adjusting the number of periods of the static electric field. In principle [11], high peak powers (MW) can be obtained over a wide wavelength range (10–100  $\mu\text{m}$ ) with varying pulse durations (1–10 ps).

In the following, we propose and analyze a device which combines some of the features of photoswitched semiconductors [1–10] and of radiation conversion using a periodic capacitor array [11]. This device will be referred to as a photoswitched periodically biased semiconductor (PPS). Radiation is generated in the PPS by applying a static, periodic electric field across the surface of a planar semiconductor (e.g., GaAs or InP). A laser pulse is injected into the device such that it propagates along and nearly parallel to the semiconductor surface, and perpendicular to the applied static field. As the pulse propagates, it generates photocarriers

<sup>\*</sup>Present address: Icarus Research, P.O. Box 30580, Bethesda, MD 20824-0780.

<sup>†</sup>Present address: Northeastern University, Department of Electrical Engineering, Boston, MA 02115.

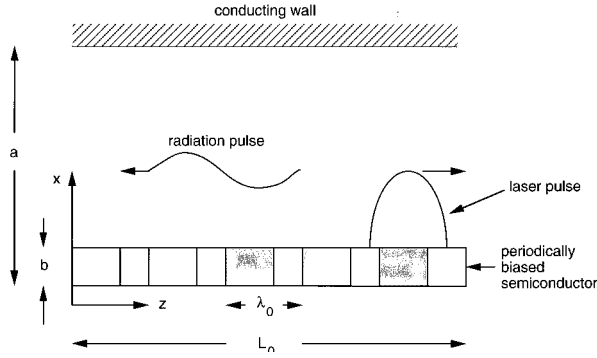


FIG. 1. Schematic of a 2D PPS device. A semiconductor wafer of thickness  $2b$  lies in the  $y,z$  plane. A conducting wall is placed parallel to the wafer at  $x=a$ . A periodic bias electric field of the form  $\mathbf{E}_b = E_0 \cos k_0 z \mathbf{e}_y$  is applied to the wafer, where  $\lambda_0 = 2\pi/k_0$  is the bias period, and  $z$  is the distance along the axis of laser propagation.

within the semiconductor and, hence, a transient current develops in response to the applied periodic electric field. These current transients generate electromagnetic radiation. A planar conductor, placed parallel to the photoconductor, can be used to confine and enhance the generated radiation (see Fig. 1).

In the one-dimensional (1D) limit, it will be shown that radiation is generated with frequency  $\omega$  given by  $\omega/c = (k_0^2 + \bar{k}_p^2)/2k_0$ , where  $k_0 = 2\pi/\lambda_0$ ,  $\lambda_0$  is the period of the static electric field,  $\bar{k}_p = \bar{\omega}_p/c$ ,  $\bar{\omega}_p = (4\pi\bar{n}_n e^2/m^*)^{1/2}$  is the effective 1D plasma frequency,  $\bar{n}_n$  is the effective 1D photocarrier density, and  $m^*$  is the effective mass of the photocarriers. In the absence of collisions,  $N_0$  periods of applied static electric field generate  $N_0$  periods of radiation. Furthermore, it will be shown that the maximum electric field of the radiation generated within the device is less than or equal to the amplitude of the applied static electric field. In the 1D limit, the maximum efficiency of converting the energy in the static electric field into electromagnetic radiation is 30%. Such a PPS device may be capable of generating hundreds of watts of coherent radiation in the 50–500- $\mu\text{m}$  range, which can be tuned by adjusting the period of the static electric field, the carrier density, and/or the device dimensions. The duration of the electromagnetic pulse can be controlled by adjusting the number of periods of the static electric field. In principle, one can choose how many cycles of radiation will be generated. Such a source of tunable, ultrashort pulse radiation would have various applications, including absorption spectroscopy, time-resolved studies in physics and chemistry, remote sensing and radar, and high-speed multiplexing.

One can envision many possible configurations for a PPS device. In this paper, we will analyze the following simplified and idealized two-dimensional (2D) configuration (see Fig. 1). Consider a single planar semiconductor, the surface of which lies in the  $y,z$  plane and is located at  $x=b$  along the  $x$  axis. A static, periodic, bias electric field of the form  $\mathbf{E}_B = E_0 \cos k_0 z \mathbf{e}_y$  is applied in the  $y$  direction, where  $k_0 = 2\pi/\lambda_0$ , and  $\lambda_0$  is the bias period. The device is of length  $L_0$  in the  $z$  direction, biased with  $N_0 = L_0/\lambda_0$  periods of static electric field, and the photoconductor is assumed to be uniform and infinite (i.e., some length  $L_y$  large compared

to other characteristic dimensions) in the  $y$  direction. To confine the generated radiation, a conducting wall is positioned at a distance  $x=a$  above and parallel to the semiconductor surface. A short laser pulse is injected between the conducting wall and the semiconductor, such that it propagates at the speed of light  $c$  in the positive  $z$  direction nearly parallel to the semiconductor, and skims along its surface. Photocarriers are assumed to be generated within a penetration depth  $b$  (between  $x=0$  and  $x=b$ ) inside the semiconductor. For simplicity, the device is assumed to be symmetric about  $x=0$ ; i.e., conducting walls are located at  $x = \pm a$ , the semiconductor is a thin slab of thickness  $2b$  centered about  $x=0$ , and laser pulses propagate along both surfaces of the semiconductor slab. In principle, one can envision using more than one semiconductor slab, placed parallel to one another, with laser pulses injected between their surfaces. The 1D limit corresponds to many closely spaced semiconductor slabs. In the following, the effects of collisional damping within the semiconductor are included; however, other nonideal effects, such as fringe electric fields or nonuniform carrier densities, are neglected.

## II. WAVE EQUATION AND CURRENT RESPONSE

The generation of electromagnetic radiation by the photoinduced current is described by the wave equation

$$\left( \nabla^2 - \frac{1}{c^2} \frac{\partial^2}{\partial t^2} \right) \mathbf{E} = \frac{4\pi}{c^2} \frac{\partial \mathbf{J}}{\partial t}, \quad (1)$$

where  $\mathbf{E}$  is the electric field generated by transients in the current density  $\mathbf{J}$ . Prior to the injection of the laser pulse, a static electric field of the form  $\mathbf{E}_B = E_0 F(z) \cos k_0 z \mathbf{e}_y$  is applied to the semiconductor sheet, where  $\lambda_0 = 2\pi/k_0$  is the wavelength of the static field,  $E_0$  is the amplitude,  $F(z) = u(z) - u(z - L_0)$ ,  $u(z)$  is the Heaviside unit step function, and  $L_0$  is the axial length of the device, i.e.,  $F(z) = 1$  for  $0 < z < L_0$  and  $F(z) = 0$  otherwise. As the laser pulse propagates along the surface of the semiconductor, it generates carriers and a photoinduced current  $\mathbf{J}$  within the semiconductor.

The following simplified model for the photoinduced current will be assumed. The photoinduced current is given by  $\mathbf{J} = -en_n v \mathbf{e}_y$ , where  $n_n$  is the effective carrier density and  $v$  is the effective carrier velocity. The carrier density is determined approximately by  $\partial n_n / \partial t = q\alpha I / \hbar \omega_L$ , where  $I$  is the laser intensity inside the semiconductor,  $\alpha$  is the absorption coefficient,  $\hbar \omega_L$  is the energy of the laser photons, and  $q$  is the quantum efficiency for converting photons into charge carriers, and the effects of diffusion and recombination have been neglected. The laser pulse duration  $\tau_L$  is assumed to be less than the characteristic response time of the device. Hence the carriers are assumed to be generated instantaneously by the laser pulse,  $n_n = n_0 u(ct - z)$ , where  $n_0 = q\alpha I \tau_L / \hbar \omega_L$  is the peak density,  $ct - z = 0$  gives the location of the laser pulse front, and the carriers exist in the region  $ct - z \geq 0$  (behind the laser pulse). Furthermore, the carrier density is assumed to be uniform within the penetration depth  $0 < |x| < b$ , i.e.,  $n_n = n_0 u(ct - z) u(b - |x|)$ .

Carriers which are produced in the presence of the electric fields  $\mathbf{E}$  and  $\mathbf{E}_B$  obey the equation

$$\frac{\partial}{\partial t}(n_n \mathbf{v}) = -\frac{en_n}{m^*}(\mathbf{E} + \mathbf{E}_B) - c\nu n_n \mathbf{v}, \quad (2)$$

where  $m^*$  is the effective mass of the carrier, and  $c\nu$  is the effective collision frequency.

Hence, the current response is given by

$$\left(\frac{\partial}{\partial t} + c\nu\right)\mathbf{J} = \frac{\omega_p^2}{4\pi}(\mathbf{E} + \mathbf{E}_B), \quad (3)$$

where  $\omega_p = (4\pi n_n e^2/m^*)^{1/2}$  is the effective plasma frequency. On the right side of Eq. (3), the electric field of the laser is neglected, i.e., it is assumed that the only role of the laser field is to generate the carrier population,  $\omega_p^2 = \omega_{p0}^2 u(ct-z)u(b-|x|)$ , where  $\omega_{p0} = (4\pi n_0 e^2/m^*)^{1/2}$ . Note that the current induced by a static, uniform electric field  $E_0$  is given by  $J = J_0[1 - \exp(-\zeta\nu)]$ , where  $J_0 = -en_n \mu E_0$  is the steady-state current,  $\mu = e/(m^*c\nu)$  is the carrier mobility,  $\zeta = ct - z$ , and  $1/c\nu$  is the relaxation time.

It is convenient to introduce the independent variables  $\zeta = ct - z$ ,  $z$ , and  $x$ . Using these variables, the 2D wave equation is given by

$$\left(\frac{\partial^2}{\partial x^2} + \frac{\partial^2}{\partial z^2} - 2\frac{\partial^2}{\partial \zeta \partial z}\right)\mathbf{E} = \frac{4\pi}{c}\frac{\partial \mathbf{J}}{\partial \zeta} \quad (4)$$

and the induced current is given by

$$\left(\frac{\partial}{\partial \zeta} + \nu\right)\mathbf{J} = \frac{\omega_p^2}{4\pi c}(\mathbf{E} + \mathbf{E}_B), \quad (5)$$

where  $\omega_p^2 = \omega_{p0}^2 u(\zeta)u(b-|x|)$ . It will also prove convenient to introduce the Laplace transform  $Q_s(s)$  of the quantity  $Q(\zeta)$  with respect to  $\zeta$ , i.e.,  $Q_s = \int_0^\infty d\zeta Q \exp(-s\zeta)$ . Taking the Laplace transform of Eqs. (4) and (5) yields the wave equation

$$\left(\frac{\partial^2}{\partial x^2} + \frac{\partial^2}{\partial z^2} - 2s\frac{\partial}{\partial z} - \frac{sk_p^2(x)}{s+\nu}\right)E_s = \frac{k_p^2(x)}{s+\nu}E_0 F(z) \cos k_0 z, \quad (6)$$

where  $E(\zeta=0) = 0$  has been assumed,  $k_p^2(x) = \omega_{p0}^2/c^2$  for  $|x| \leq b$ , and  $k_p^2(x) = 0$  for  $|x| > b$ ; i.e., the charge carriers only exist within the semiconductor of thickness  $2b$ . Within the region of the semiconductor,  $0 < z < L_0$ , the device is periodic in  $z$  and the induced electric field can be written as the real part of  $E_s = \hat{E}_s \exp(ik_0 z)$ . Hence the wave equation becomes

$$\left(\frac{\partial^2}{\partial x^2} - k_0^2 - 2isk_0 - \frac{sk_p^2(x)}{s+\nu}\right)\hat{E}_s = \frac{k_p^2(x)}{s+\nu}E_0. \quad (7)$$

### III. ONE-DIMENSIONAL LIMIT

To gain an understanding of the basic mechanism of radiation generation and the characteristics of the radiation (e.g., the wavelength, group velocity, pulse duration, etc.), it is insightful to solve Eq. (7) in the one-dimensional (1D) limit. The 1D limit is obtained by letting  $\partial/\partial x \rightarrow 0$  and  $k_p(x) \rightarrow \bar{k}_p$  in Eq. (7), where  $\bar{k}_p$  is the effective 1D plasma

wave number and is constant. The 1D limit corresponds to a PPS device consisting of many thin semiconductor wafers placed closely together. In this case, the effective 1D plasma wave number is given by  $\bar{k}_p^2 \approx \delta_1 k_p^2/\Delta$ , where  $\delta_1$  is the wafer thickness and  $\Delta$  is the separation between wafers. In effect, the laser pulse is propagating through a uniform, continuous medium producing photoconductors characterized by a plasma wave number  $\bar{k}_p$ . The 1D limit is also directly applicable to the case of a photoionized gas [11], i.e., the laser pulse propagates into a gas with a periodic static electric field and ionizes the gas to produce a plasma with a plasma frequency  $c\bar{k}_p$ . Since the ionizing laser is assumed to propagate with velocity  $c$ , it is implicitly assumed that  $\omega_L \gg c\bar{k}_p$ , where  $\omega_L$  is the frequency of the ionizing laser.

In the 1D limit, the wave equation, Eq. (7), becomes

$$[(2isk_0 + k_0^2)(s + \nu) + s\bar{k}_p^2]\hat{E}_s = -\bar{k}_p^2 E_0. \quad (8)$$

Hence  $\hat{E}_s = -\bar{k}_p^2 E_0/D(s)$ , where the 1D dispersion relation is given by

$$D(s) = (2isk_0 + k_0^2)(s + \nu) + s\bar{k}_p^2. \quad (9)$$

The inverse Laplace transform is governed by the zeros of  $D(s)$ . Equation (9) can be written as  $D = 2ik_0(s - s_1)(s - s_2)$ , where  $s_{1,2}$  are the zeros of  $D(s)$  given by

$$s_{1,2} = -\frac{\nu}{2} + \frac{i}{4k_0}(k_0^2 + \bar{k}_p^2) \pm \frac{1}{2} \left\{ \left[ \nu - \frac{i}{2k_0}(k_0^2 + \bar{k}_p^2) \right]^2 + 2ik_0\nu \right\}^{1/2}. \quad (10)$$

The inverse transform of  $\hat{E}_s$  is given by

$$\hat{E}(\zeta) = \frac{ik_p^2 E_0}{2k_0(s_1 - s_2)} [\exp(s_1 \zeta) - \exp(s_2 \zeta)]. \quad (11)$$

Equations (10) and (11) can be analyzed in various limits.

In the absence of collisions,  $\nu = 0$ , the zeros are  $s_1 = i(k_0^2 + \bar{k}_p^2)/2k_0$  and  $s_2 = 0$ . Hence  $E = \hat{E} \exp(ik_0 z)$  is given by

$$E = \frac{\bar{k}_p^2 E_0}{(\bar{k}_p^2 + k_0^2)} \left\{ \exp \left[ \frac{i}{2k_0}(\bar{k}_p^2 + k_0^2)\zeta + ik_0 z \right] - \exp(ik_0 z) \right\}. \quad (12)$$

The first term on the right of Eq. (12) represents the induced electromagnetic wave, and the second term represents an induced static electric field. The electric field of the electromagnetic wave can be written in terms of  $z$  and  $t$  as

$$E = \frac{\bar{k}_p^2 E_0}{(\bar{k}_p^2 + k_0^2)} \exp[i(\omega t - k_z z)], \quad (13)$$

where the axial wave number and frequency are given by

$$k_z = (\bar{k}_p^2 - k_0^2)/2k_0, \quad (14)$$

$$\omega/c = (\bar{k}_p^2 + k_0^2)/2k_0, \quad (15)$$

respectively. Notice that  $\omega^2/c^2 = k_z^2 + \bar{k}_p^2$ , which is the dispersion relation for electromagnetic radiation propagating in a plasma with a plasma frequency  $c\bar{k}_p$ . Since the frequency of the radiation remains constant as the radiation exits the device, the wavelength of the generated radiation is  $\lambda = 2\pi c/\omega$ . Also notice that the electric field amplitude of the radiation is maximum when  $\bar{k}_p^2 \gg k_0^2$ , and equal to the bias electric field amplitude  $E_0$ .

Within the device, the axial group velocity  $v_g$  and axial phase velocity  $v_p$  of the radiation are related by  $v_p/c = \omega/c k_z = c/v_g$ . Hence the axial group velocity is given by

$$v_g/c = (\bar{k}_p^2 - k_0^2)/(\bar{k}_p^2 + k_0^2). \quad (16)$$

In the limit  $\bar{k}_p^2 \ll k_0^2$ , the radiation wavelength is  $\lambda = 2\pi c/\omega \approx 4\pi/k_0 = 2\lambda_0$ , and the group velocity is  $v_g \approx -c$ , i.e., the wavelength is twice that of the static electric field and is moving in the negative  $z$  direction (the direction opposite of the incident laser pulse) at approximately the speed of light  $c$ . In the limit  $\bar{k}_p^2 \gg k_0^2$ , the radiation wavelength is  $\lambda \approx 2\lambda_0 k_0^2/\bar{k}_p^2 \ll 2\lambda_0$ , and the group velocity is  $v_g \approx c(1 - 2k_0^2/\bar{k}_p^2)$ , i.e., the wave is moving in the positive  $z$  direction (the direction of the incident laser pulse) at approximately the speed of light  $c$ . Notice that when  $\bar{k}_p = k_0$ ,  $k_z \rightarrow 0$  and  $v_g \rightarrow 0$ , i.e., the wave has a time dependence only with frequency  $\omega = ck_0$ , and no energy leaves the device.

The length  $L$  of the electromagnetic pulse generated by the device can be determined as follows. The incident laser pulse encounters the periodic static electric field at  $z=0$  and  $t=0$ , at which point the radiation begins to be generated. The time it takes the laser pulse to reach the end of the periodic structure ( $z=L_0$ ) is given by  $T=L_0/c$ . During this time the ‘‘front’’ of the radiation pulse, which was generated at  $z=0$ , has traveled a distance  $v_g T = L_0 v_g/c$  and is now located at  $z=L_0 v_g/c$ . Since the ‘‘back’’ of the radiation pulse at time  $t=T$  is located at  $z=L_0$ , the total length of the radiation pulse is given by  $L = (1 - v_g/c)L_0$ . Hence,

$$L = \frac{2k_0^2 L_0}{(\bar{k}_p^2 + k_0^2)}, \quad (17)$$

or  $L = ck_0 L_0/\omega$ . Since the wavelength of the radiation existing in the device is  $\lambda = 2\pi c/\omega$ ,  $L = \lambda L_0/\lambda_0$ . In terms of the number of periods of the radiation pulse,  $N = L/\lambda$ , and the number of periods of the static electric field,  $N_0 = L_0/\lambda_0$ ,  $N = N_0$ . In other words, a device consisting of  $N_0$  periods of a static, sinusoidal electric field of wavelength  $\lambda_0$  will generate  $N_0$  periods of radiation of wavelength  $\lambda = 2\pi c/\omega$ , where  $\omega$  is given by Eq. (15). Within the device, the pulse is traveling with a group velocity given by Eq. (16). For example, in the limit  $\bar{k}_p^2 \ll k_0^2$ ,  $v_g \approx -c$  (the radiation is traveling opposite to the incident laser pulse),  $\lambda \approx 2\lambda_0$ , and  $L \approx 2L_0$ . In the limit  $\bar{k}_p^2 \gg k_0^2$ ,  $v_g \approx c(1 - 2k_0^2/\bar{k}_p^2)$  (the radiation is traveling in the direction of the incident laser pulse),  $\lambda \approx 2\lambda_0 k_0^2/\bar{k}_p^2$ , and  $L \approx 2L_0 k_0^2/\bar{k}_p^2$ .

The average intensity, or power flux, of the radiation within the device is given by  $I = \langle |\mathbf{S}| \rangle$ , where  $\mathbf{S} = c(\mathbf{E} \times \mathbf{B})/4\pi$  is the Poynting flux, and the angular brackets

signify a time average. In the 1D limit,  $\mathbf{S} = (v_g E^2/4\pi)\mathbf{e}_z$ . Hence  $I = |v_g| |E|^2/8\pi$ , or

$$I = \frac{c}{8\pi} \frac{\bar{k}_p^2 |\bar{k}_p^2 - k_0^2|}{(\bar{k}_p^2 + k_0^2)^3} E_0^2. \quad (18)$$

The power exiting the device is  $P = IL_x L_y$ , where  $L_x$  and  $L_y$  are the  $x$  and  $y$  device dimensions. Notice that the intensity (power) is maximum when  $\bar{k}_p^2 \gg k_0^2$ , and is given by  $I = cE_0^2/8\pi$ . The total energy  $W$  in the radiation pulse is found by multiplying  $P$  by the pulse length  $L/c$ , Eq. (17), i.e.,  $W = IL_x L_y L/c$ . In terms of the total energy in the static electric field initially stored within the device,  $W_0 = (E_0^2/16\pi)L_x L_y L_0$ , the total pulse energy is given by

$$W = \frac{4k_0^2 \bar{k}_p^4 |\bar{k}_p^2 - k_0^2|}{(\bar{k}_p^2 + k_0^2)^4} W_0. \quad (19)$$

The energy conversion efficiency  $\eta = W/W_0$  is maximum when  $\bar{k}_p^2 = (5 + \sqrt{17})k_0^2/2$ , which implies  $\lambda \approx (0.6)^2 \lambda_0$  and  $W/W_0 \approx 31\%$ .

The above results have assumed  $\nu = 0$ . In the limit of weak collisional damping,  $\nu \ll (\bar{k}_p^2 + k_0^2)/2k_0$ , the two roots are given by

$$s_1 = \frac{i}{2k_0} (\bar{k}_p^2 + k_0^2) - \frac{\nu \bar{k}_p^2}{(\bar{k}_p^2 + k_0^2)}, \quad (20)$$

and  $s_2 = -\nu k_0^2/(\bar{k}_p^2 + k_0^2)$ . The above results, Eqs. (12)–(19), still apply, only now the mode is damped in  $\zeta$ , i.e., the electric field, Eq. (13), is multiplied by the damping factor  $\exp(-\zeta/L_d)$ , where the damping distance  $L_d$  is given by  $L_d^{-1} = \nu k_0^2/(\bar{k}_p^2 + k_0^2)$ . In effect, this limits the length of the radiation pulse,  $L \lesssim L_d$ .

In the limit of strong collisional damping,  $\nu \gg (\bar{k}_p^2 + k_0^2)/2k_0$ , the two roots are given by  $s_1 \approx ik_0/2 - \bar{k}_p^2/4\nu$  and  $s_2 \approx -\nu$ . The electric field of the radiation is given by

$$E \approx \frac{i\bar{k}_p^2 E_0}{2\nu k_0} \exp\left[\left(i\frac{k_0}{2} - \frac{\bar{k}_p^2}{4\nu}\right)\zeta + ik_0 z\right]. \quad (21)$$

The frequency, axial wave number, and group velocity of the mode are  $\omega/c = k_0/2$ ,  $k_z = -k_0/2$ , and  $v_g \approx -c$ . Notice that in the strong damping limit, the amplitude of the electric field is reduced by the factor  $[(\bar{k}_p^2 + k_0^2)/(2k_0\nu)]\exp(-\zeta/L_d)$  compared to Eq. (13), where the damping distance is  $L_d^{-1} = 4\nu\bar{k}_p^2$ . Hence the intensity  $I$  and the total pulse energy  $W$  are reduced by  $(\bar{k}_p^2 + k_0^2)^2/(2k_0\nu)^2$ , and the length of the radiation pulse is limited to  $L \lesssim L_d$ .

#### IV. TWO-DIMENSIONAL SOLUTIONS

The generation of radiation in 2D can be described by solving Eq. (7) inside and outside the semiconductor. Within the semiconductor,  $|x| < b$ , the Laplace transform of the electric field is given by  $\hat{E}_s = \hat{E}_{s1} = F + A_1 \cos k_1 x$ , and outside,  $b < |x| < a$ ,  $\hat{E}_s = \hat{E}_{s2} = A_2 \sin k_2(a-x)$ , where

$$k_1^2 = -2ik_0s - k_0^2 - sk_p^2/(s + \nu), \quad (22)$$

$$k_2^2 = -2ik_0s - k_0^2, \quad (23)$$

$F = (k_p/k_1)^2 E_0/(s + \nu)$ , and  $A_{1,2}$  are constants (independent of  $x$ ). The functional forms of  $E_{s1,2}$  have assumed the boundary conditions  $\partial E_s/\partial x = 0$  at  $x = 0$  and  $E_s = 0$  at  $x = a$ , i.e., the symmetric solution. The coefficients  $A_{1,2}$  can be found by requiring  $E_s$  and  $\partial E_s/\partial x$  to be continuous at  $x = b$ . This gives

$$\hat{E}_{s1} = F[1 + D^{-1}k_2 \cos k_2(a - b) \cos k_1 x], \quad (24)$$

$$\hat{E}_{s2} = FD^{-1}k_1 \sin k_1 b \sin k_2(a - x), \quad (25)$$

where the dispersion relation  $D(s)$  is given by

$$D(s) = k_1 \sin k_2(a - b) \sin k_1 b - k_2 \cos k_2(a - b) \cos k_1 b. \quad (26)$$

The inverse Laplace transform of Eqs. (24) and (25) is determined largely by the zeros of  $D(s)$ , i.e.,  $s = s_n$ , where  $D(s_n) = 0$ . Near a zero,  $D \approx (s - s_n) \partial D/\partial s$ . Using standard theory of residues and assuming simple poles, the asymptotic behavior of the inverse transform of the electric field is given by

$$E_1 = \sum_n \frac{k_p^2 b E_0 \sin k_2(a - b)}{(s_n + \nu) \partial D/\partial s} \cos k_1 x \exp(s_n \zeta + ik_0 z), \quad (27)$$

$$E_2 = \sum_n \frac{k_p^2 b E_0}{(s_n + \nu) \partial D/\partial s} \sin k_2(a - x) \exp(s_n \zeta + ik_0 z), \quad (28)$$

where the right side is evaluated at  $s = s_n$ , and the sum is over all zeros  $s_n$ . For the modes of interest,  $s_n$  can be written as  $s_n = ik_n - \gamma_n$ , where  $\gamma_n$  is the damping rate,  $\omega_n = ck_n$  is the frequency,  $k_z = k_n - k_0$  is the axial wave number, and  $v_g = c^2 k_z/\omega_n$  is the axial group velocity.

In the limit  $b \ll a$ , the total power is dominated by the field  $E_2$  in the region  $b < |x| < a$ . The intensity of the radiation  $I = c \langle |\mathbf{E} \times \mathbf{B}| \rangle / 4\pi$  is given by  $I \approx c^2 |v_g| |E_2|^2 / 8\pi$  and the power is  $P \approx L_y \int dx I$ . Hence the power in the  $n$ th mode can be written as

$$P_n \approx \frac{caL_y |k_n - k_0|}{8\pi k_n} \left| \frac{bk_p^2 E_0}{(s_n + \nu) \partial D/\partial s} \right|^2 \exp(-2\gamma_n \zeta). \quad (29)$$

In the absence of collisions ( $\nu = 0$ ,  $\gamma_n = 0$ ), the pulse length of the radiation is given by  $L_n \approx (1 - v_g/c)L_0$ , where  $v_g = c^2 k_z/\omega_n = c(k_n - k_0)/k_n$  is the axial group velocity. Hence  $L_n \approx k_0 L_0/k_n$ , i.e., a device consisting of  $N_0 = L_0/\lambda_0$  periods of bias field will produce a radiation pulse consisting of  $N = N_0$  periods of radiation, where  $N = L_n/\lambda$ ,  $\lambda = 2\pi c/\omega_n$ , and  $\omega_n = ck_n$ . The total energy in the  $n$ th mode radiation pulse is given by  $W_n \approx P_n L_n/c \approx (k_0/k_n) P_n L_0/c$ , where  $P_n$  is given by Eq. (29) with  $\gamma_n = 0$ .

To further evaluate the inverse Laplace transforms, Eqs. (27) and (28), it is necessary to find the zeros of  $D(s)$ . Insight can be gained by noting that in either the limit  $k_p \rightarrow 0$  or

$b \rightarrow 0$ ,  $D = -k_2 \cos k_2 a$ . In these limits,  $D = 0$  implies  $k_2 = (2l + 1)\pi/2a$ , where  $l$  is an integer. Hence, the zeros of  $D(s)$  are given by  $s = s_n$ , where  $s_n = i(k_0^2 + k_x^2)/2k_0$ ,  $k_x = n\pi/2a$ , and  $n = 2l + 1$  is odd. This implies the radiation is generated in discrete modes, where the frequency of the  $n$ th mode is  $\omega_n = -is_n$ .

A more relevant limit can be analyzed in the limit of a thin current sheet  $b/a \ll 1$  by assuming  $|k_{1,2}b| \ll 1$ . Then,

$$D \approx -\hat{k}_p^2 b \sin k_2 a - k_2 \cos k_2 a, \quad (30)$$

where  $\hat{k}_p^2 = sk_p^2/(s + \nu)$ . Notice that  $|\hat{k}_p^2 b^2| \ll 1$  is implied by  $|k_{1,2}b| \ll 1$ , and that  $\hat{k}_p = k_p$  in the absence of collisions ( $\nu = 0$ ). The zeros of  $D(k_2) = 0$  can be approximated by letting  $k_2 = k_x + \delta k_x$ , and assuming  $|\delta k_x a| \ll 1$ . Analytical expressions for the quantities  $k_x$  and  $\delta k_x$  can be found in various limits, specifically when (A)  $|\hat{k}_p^2 ab| \ll 1$  and (B)  $|\hat{k}_p^2 ab| \gg 1$ .

Consider the limit (A)  $|\hat{k}_p^2 ab| \ll 1$ . Notice that this, along with  $|\hat{k}_p^2 b^2| \ll 1$ , imply  $|\hat{k}_p^2 b^2| \ll b/a \ll 1$ . In this limit, the zeros of  $D(k_2)$ , Eq. (30), are given by  $k_2 = k_{x1} + \delta k_{x1}$ , where  $k_{x1} = n\pi/2a$ ,  $n = 2l + 1$  is odd, and  $\delta k_{x1} \approx b\hat{k}_p^2/k_{x1}a$ . Using the definition of  $k_2$ , the zeros of  $D(s)$  are given by  $s = s_n$ , where

$$2s_n = -\nu + ik_t \pm \left[ (\nu - ik_t)^2 + \frac{2i\nu}{k_0} (k_0^2 + k_{x1}^2) \right]^{1/2}, \quad (31)$$

and  $k_t = (k_0^2 + k_{x1}^2 + 2bk_p^2/a)/2k_0$ . Notice that this reduces to the 1D limit when  $k_{x1} = 0$  and  $2bk_p^2/a = \bar{k}_p^2$ . Furthermore,  $\partial D/\partial s \approx i(-1)^l a k_0$ . Simplified expressions for the zeros, Eq. (31), can be found in the limits of weak,  $\nu \ll k_t$ , or strong,  $\nu \gg k_t$ , collisions. The zeros can be written as  $s_n = ik_n - \gamma_n$ , where the mode frequency  $\omega_n = ck_n$  and damping rate  $\gamma_n$  are given by

$$k_n = \begin{cases} (k_0^2 + k_{x1}^2 + 2bk_p^2/a)/2k_0 & \text{for } \nu \ll k_t, \\ (k_0^2 + k_{x1}^2)/2k_0 & \text{for } \nu \gg k_t \end{cases} \quad (32)$$

and

$$\gamma_n = \begin{cases} \nu bk_p^2/ak_0 k_n & \text{for } \nu \ll k_t \\ bk_n k_p^2/a \nu k_0 & \text{for } \nu \gg k_t. \end{cases} \quad (33)$$

The power in the  $n$ th mode can be written, in the limit  $|\hat{k}_p^2 ab| \ll 1$ , as

$$P_n \approx \frac{caL_y |k_n - k_0|}{8\pi k_n (k_n^2 + \nu^2)} \left( \frac{bk_p^2 E_0}{k_0 a} \right)^2 \exp(-2\gamma_n \zeta), \quad (34)$$

where  $k_n$  and  $\gamma_n$  are given by Eqs. (32) and (33) in the appropriate limits. Equation (34) indicates that the power in the various modes increases with increasing  $k_p$ . In fact, when  $\nu = 0$ , the expression for the power becomes independent of  $k_p$  for sufficiently large  $k_p$ . However, Eq. (34) assumed that  $|\hat{k}_p^2 ab| \ll 1$ ; i.e., it is not valid in the large  $k_p$  limit.

Consider the limit (B)  $|\hat{k}_p^2 ab| \gg 1$ . Notice that this along with  $|\hat{k}_p^2 b^2| \ll 1$  imply  $b/a \ll |\hat{k}_p^2 b^2| \ll 1$ . In this limit, the zeros of  $D(k_2)$ , Eq. (30), are given by  $k_2 = k_{x2} + \delta k_{x2}$ , where  $k_{x2} = l\pi/a$  ( $l$  is an integer) and  $\delta k_{x2} \approx -k_{x2}/\hat{k}_p^2 ab$ . Hence  $s_n = ik_n - \gamma_n$ , where the frequency  $\omega_n = ck_n$  and damping rate  $\gamma_n$  are given by

$$k_n = (k_0^2 + k_{x2}^2)/2k_0, \quad (35)$$

$$\gamma_n = \nu k_{x2}^2 / abk_0 k_n k_p^2. \quad (36)$$

Furthermore,  $\partial D/\partial s \approx (-1)^l i abk_0 \hat{k}_p^2 / k_{x2}$ . The power in the  $n$ th mode can be written as

$$P_n \approx \frac{caL_y k_{x2}^4 |k_{x2}^2 - k_0^2| E_0^2}{2\pi^3 l^2 (k_{x2}^2 + k_0^2)^3} \exp(-2\gamma_n \xi). \quad (37)$$

Since the axial wave number of the mode is  $k_z = k_n - k_0$ , the axial group velocity is  $v_g/c = (k_{x2}^2 - k_0^2)/(k_{x2}^2 + k_0^2)$ . The length of the radiation pulse is approximately  $L_n \approx (1 - v_g/c)L_0$ , which gives  $L_n \approx 2k_0^2 L_0 / (k_{x2}^2 + k_0^2)$ , assuming  $L_n \leq 1/2\gamma_n$ . Neglecting collisions,  $\nu \rightarrow 0$ , the total energy in the  $n$ th mode is  $W_n \approx P_n L_n / c$ , which gives

$$W_n \approx \frac{8k_0^2 k_{x2}^4 |k_{x2}^2 - k_0^2|}{\pi^2 l^2 (k_{x2}^2 + k_0^2)^4} W_0, \quad (38)$$

where  $W_0$  is defined as  $W_0 = aL_y L_0 E_0^2 / 8\pi$ , i.e., the energy density of the electrostatic field multiplied by the device volume. As with the 1D limit,  $W_n/W_0$  is maximum when  $k_{x2}^2 = (5 + \sqrt{17})k_0^2/2$ , i.e., when  $a/l \approx 0.16\lambda_0$ . This corresponds to a wavelength  $\lambda_1 = 2\pi c/\omega_1 \approx 0.36\lambda_0$  and a maximum efficiency of  $W_n/W_0 \approx (6.3/l^2)\%$ .

## V. NUMERICAL EXAMPLES

The analytic expressions presented in Sec. IV for the mode frequency  $\omega_n = ck_n$ , the damping rate  $\gamma_n$ , and the power  $P_n$  were based on solving the simplified dispersion relation, Eq. (30), in the limit  $|\hat{k}_p b|^2 \ll 1$ . To verify the analytic theory, the zeros of the full dispersion relation, Eq. (26), were found numerically as a function of  $k_p^2 \propto n_0$ , where  $n_0$  is the density of charge carriers. The numerical solutions assumed a current layer thickness of  $b = 1 \mu\text{m}$ , a conducting wall located at  $a = 100 \mu\text{m}$ , a bias field period of  $\lambda_0 = 400 \mu\text{m}$ , and a collision frequency  $c\nu$  given by  $\nu^{-1} = 100 \mu\text{m}$ . The effective plasma frequency  $\omega_p = ck_p$  was varied over the range  $1 \text{ cm}^{-1} < k_p < 10^5 \text{ cm}^{-1}$ .

The lowest order zero to Eq. (26),  $s = s_1$ , is plotted in Fig. 2, where  $s_1 = ik_1 - \gamma_1$ . The mode wave number  $k_1$  is given by the imaginary part of  $s_1$ , which is plotted in Fig. 2(a). Notice that in the limit  $k_p \rightarrow 0$ , Eq. (32) predicts that  $k_1 \approx (k_0^2 + k_{x1}^2)/2k_0 \approx 157 \text{ cm}^{-1}$ , which is in agreement with Fig. 2(a). In the limit  $abk_p^2 \gg 1$  ( $k_p \gg 10^3 \text{ cm}^{-1}$ ), Eq. (35) predicts that  $k_1 \approx (k_0^2 + k_{x2}^2)/2k_0 \approx 393 \text{ cm}^{-1}$ , again in agreement with Fig. 2(a). The damping rate is given by the real part of  $s_1$ , which is plotted in Fig. 2(b). A maximum value of  $\gamma_1 = 24 \text{ cm}^{-1}$  ( $\gamma_1^{-1} = 420 \mu\text{m}$ ) is obtained at  $k_p \approx 1.5 \times 10^3 \text{ cm}^{-1}$ . Away from this value, i.e.,  $k_p \ll 10^3$

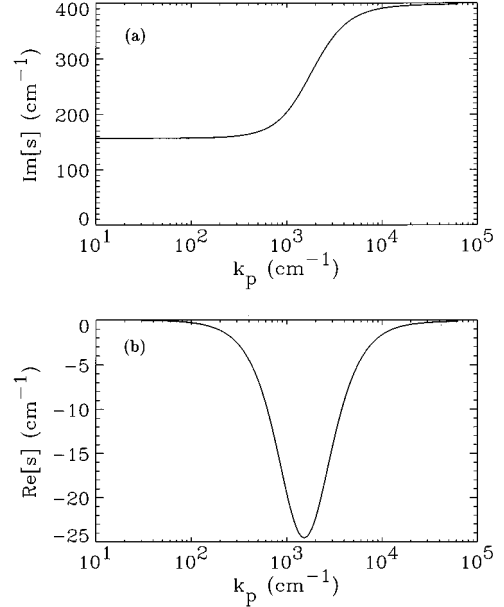


FIG. 2. Numerical solution to the 2D dispersion relation, Eq. (26), for the parameters  $b = 1 \mu\text{m}$ ,  $a = 100 \mu\text{m}$ ,  $\lambda_0 = 400 \mu\text{m}$ , and  $\nu^{-1} = 100 \mu\text{m}$ . The lowest order zero  $s_1 = ik_1 - \gamma_1$  is plotted as a function of  $k_p$ . (a) shows the imaginary part of  $s_1$ , i.e., the mode frequency  $\omega_1 = ck_1$ , and (b) shows the real part of  $s_1$ , i.e., the damping rate  $\gamma_1 = L_d^{-1}$ .

$\text{cm}^{-1}$  or  $k_p \gg 10^3 \text{ cm}^{-1}$ ,  $\gamma_1$  rapidly diminishes, as predicted by Eqs. (33) and (36).

The real and imaginary parts of  $\partial D/\partial s$ , evaluated at  $s = s_1$ , are shown in Figs. 3(a) and 3(b), respectively. These quantities are important for determining the radiation power, as indicated by Eq. (29). It is useful to define a normalized power

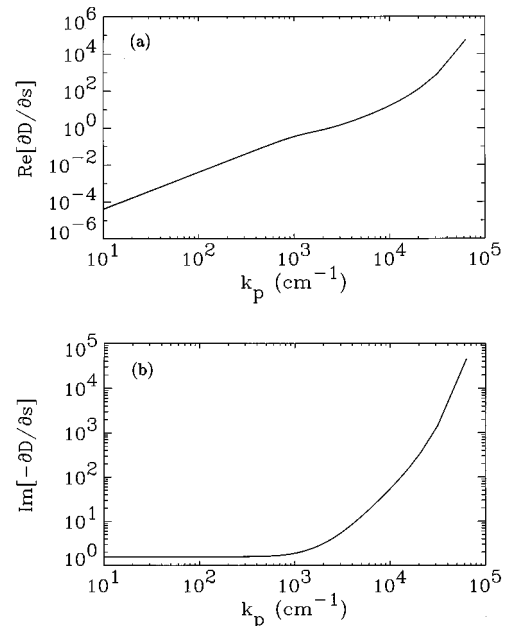


FIG. 3. The (a) real and (b) imaginary parts of  $\partial D/\partial s$ , evaluated at  $s = s_1$ , vs  $k_p$ , for the parameters of Fig. 2.

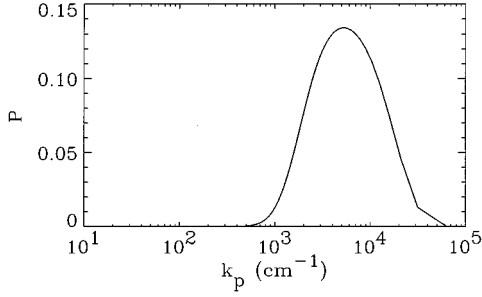


FIG. 4. The normalized power,  $\hat{P}_1$ , Eq. (39), evaluated at  $s=s_1$ , vs  $k_p$ , for the parameters of Fig. 2.

$$\hat{P}_n = \left| \frac{(k_n - k_0) b k_p^2}{k_n (s_n + \nu) \partial D / \partial s} \right|^2, \quad (39)$$

where the maximum power in the  $n$ th mode is given by  $P_n = (caL_y E_0^2 / 8\pi) \hat{P}_n$ . The quantity  $\hat{P}_1$ , evaluated at  $s_n = ik_1 - \gamma_1$ , is plotted in Fig. 4 as a function of  $k_p$ . Figure 4 shows that the power achieves a maximum of  $\hat{P}_1 = 0.135$  at a value of  $k_p \approx 5 \times 10^3 \text{ cm}^{-1}$ . At  $k_p \approx 5 \times 10^3 \text{ cm}^{-1}$ , where the power is maximum, the mode frequency  $ck_1$  is given by  $k_1 = 375 \text{ cm}^{-1}$  (a wavelength of  $\lambda_1 = 2\pi/k_1 = 168 \text{ }\mu\text{m}$ ), and the damping rate is  $\gamma_1 \approx 6 \text{ cm}^{-1}$  ( $\gamma_1^{-1} = 0.17 \text{ cm}$ ). In the limit  $k_p^2 ab \gg 1$  ( $k_p > 10^3 \text{ cm}^{-1}$ ), theory predicts

$$\hat{P}_1 = \frac{4k_{x2}^2 |k_{x2}^2 - k_0^2|}{a^2 (k_{x2}^2 + k_0^2)^3}, \quad (40)$$

as indicated by Eq. (37). For the values used in Fig. 4 ( $a = 100 \text{ }\mu\text{m}$ ,  $k_{x1} = 314 \text{ cm}^{-1}$ , and  $k_0 = 157 \text{ cm}^{-1}$ ),  $\hat{P}_1 \approx 0.156$ , somewhat greater (15%) than the numerical maximum.

As an example, consider a device with a conducting wall at  $a = 100 \text{ }\mu\text{m}$ , a width of  $L_y = 1 \text{ cm}$ , and a GaAs semiconductor with a photoinduced current thickness of  $b = 1 \text{ }\mu\text{m}$ . The applied static electric field has an amplitude of  $E_0 = 10 \text{ kV/cm}$  and a period of  $\lambda_0 = 400 \text{ }\mu\text{m}$ . The carrier mobility for GaAs is  $\mu_n = 8500 \text{ cm}^2/\text{V s}$ , which gives an effective collision frequency  $c\nu = e/m^* \mu_n$  of  $1/c\nu = 0.32 \text{ ps}$  or  $1/\nu = 96 \text{ }\mu\text{m}$ , where  $m^*$  is the effective mass of the carriers ( $m^*/m_e = 0.067$  for GaAs). These values are nearly identical to those used in Figs. 2–4. A value of  $abk_p^2 = 25$  is assumed, i.e.,  $k_p \approx 5 \times 10^3 \text{ cm}^{-1}$ , which is the value at which the power is maximum in Fig. 4. This corresponds to a carrier density  $n_n = 4.7 \times 10^{17} \text{ cm}^{-3}$  (recall that  $k_p^2 = 4\pi n_n e^2 / m^* c^2$ ). From Figs. 2–4,  $k_1 \approx 375 \text{ cm}^{-1}$ ,  $\gamma_1 \approx 5.8 \text{ cm}^{-1}$ , and  $\hat{P}_1 \approx 0.135$ . This corresponds to a radiation wavelength of  $\lambda_1 = 2\pi/k_1 \approx 170 \text{ }\mu\text{m}$ , a damping length of  $\gamma_1^{-1} \approx 0.17 \text{ cm}$ , and a peak radiation power of  $P_1 \approx 180 \text{ W}$ . In the absence of collisions, a device consisting of  $N_0$  periods of static field produces  $N_0$  periods of radiation. The radiation pulse length would be  $L = N_0 \lambda$ . However, for this example, collisions limit the radiation pulse length to  $L \lesssim \gamma_1^{-1}$ . This limits the number of radiation periods to  $N \lesssim (\gamma_1 \lambda)^{-1} \approx 10$ , i.e., because of collisions, the device needs to consist of  $N_0 \leq 10$  static field periods. This gives a radiation pulse duration of  $L/c \lesssim 5.7 \text{ ps}$ . A carrier population of  $n_n = 4.7 \times 10^{17} \text{ cm}^{-3}$

can be produced with a  $0.5\text{-}\mu\text{m}$ ,  $100\text{-fs}$  laser pulse of intensity  $\sim 10^8 \text{ W/cm}^2$ , as implied by the relation  $n_n = q\alpha I \tau_L / \hbar \omega_L$  (see Sec. II), assuming  $q = 1$  and an absorption coefficient of  $\alpha = 10^4 \text{ cm}^{-1}$ . The laser power absorbed in producing this carrier population is  $\sim 100 \text{ kW}$ . Hence a laser pulse energy  $\sim 1 \text{ }\mu\text{J}$  should be sufficient.

## VI. DISCUSSION

A PPS (photoswitched periodically biased semiconductor) device has been proposed and analyzed as a compact source of short-pulse, tunable, far-infrared radiation. The analysis assumed a simplified geometry, shown in Fig. 1, which consists of a planar semiconductor (in the  $y, z$  plane) biased with a periodic electric field of the form  $\mathbf{E}_B = E_0 \cos k_0 z \mathbf{e}_y$ . A laser pulse is injected into the device, such that it propagates in the  $z$  direction, skimming along the surface of the wafer. The laser pulse produces photocarriers and a transient current response, leading to the generation of far-infrared radiation. A conducting wall, placed parallel to the wafer at a separation distance of  $x = a$ , is used to confine the radiation.

The PPS concept combines of the features of radiation generation by optical switching of a biased semiconductor [1–10], and of radiation generation using an ionization front in a periodically biased gas [11]. High-power, subpicosecond, half-cycle radiation pulses have been generated by illuminating a GaAs wafer that is biased with a uniform field. You *et al.* [7] report a maximum pulse power of  $\sim 100 \text{ kW}$  per  $\text{cm}^2$  of GaAs with a bias field of  $\sim 10 \text{ kV/cm}$  when illuminated at normal incidence by a  $120\text{-fs}$  laser with a fluence of  $\sim 40 \text{ }\mu\text{J/cm}^2$ . Froberg *et al.* [5] used a similar experimental arrangement; however, the GaAs wafer was biased with a periodic field of the form  $\mathbf{E}_B = E_0 \cos k_0 z \mathbf{e}_z$ , with a bias period on the order of  $1 \text{ mm}$  (by contrast, the PPS uses a bias field of the form  $\mathbf{E}_B = E_0 \cos k_0 z \mathbf{e}_y$ ). As with Ref. [7], no conducting wall was present, and the semiconductor was illuminated at angles near normal to the wafer. When illuminated at an angle of  $\phi$  from normal, the time dependence of the electric field of the radiation observed at an angle of  $\theta$  from normal scales [5] approximately as  $\cos \theta (\sin \theta + \sin \phi)^{-1} E_0 \cos [ck_0 t (\sin \theta + \sin \phi)^{-1}]$ , i.e., the frequency of the radiation is given by  $ck_0 (\sin \theta + \sin \phi)^{-1}$ . Except for the bias period  $k_0$ , the radiation frequency is independent of the properties of the semiconductor, in contrast to a PPS in which the frequency is a function of the carrier density. For a given incident laser spot size, the radiation pulse duration can be estimated from geometric arguments. Froberg *et al.* [5] measured a radiated power of  $\sim 10 \text{ nW}$  per  $\text{cm}^2$  of wafer for a bias field of a few  $\text{kV/cm}$  and a laser fluence of  $10 \text{ nJ/cm}^2$ . The radiated power scales roughly as  $P_{\text{rad}} \sim P_{\text{opt}}^2 E_0^2$  for laser fluences  $< 1 \text{ }\mu\text{J/cm}^2$  and  $E_0 < 10 \text{ kV/cm}$ , where  $P_{\text{opt}}$  is the incident laser power. This scaling predicts radiated powers on the order of  $100 \text{ }\mu\text{W}$  per  $\text{cm}^2$  of wafer for an incident laser fluence of  $1 \text{ }\mu\text{J/cm}^2$ .

Mori *et al.* [11] proposed radiation generation by using a parallel capacitor array to bias a gas with a periodic field of the form  $\mathbf{E}_B = E_0 \cos k_0 z \mathbf{e}_y$ . An intense laser pulse propagating along the  $z$  axis ionizes the gas to produce radiation at a frequency given by  $\omega \approx c(k_0^2 + k_p^2) / 2k_0$ , where  $\omega_p = ck_p$  is the electron plasma frequency. In the absence of collisions,  $N_0$  periods of bias field produce  $N_0$  periods of radiation.

Generation of radiation in the 10–100- $\mu\text{m}$  range may be possible. One potential disadvantage of this scheme is that it requires high laser intensity. Rapid ionization of the gas can require laser intensities on the order of  $10^{14}$  W/cm<sup>2</sup>. Hence a 1-J, 1-ps laser pulse can ionize a cross-sectional area of approximately  $(1\text{ mm})^2$ . This implies a radiated power on the order of few kW. A PPS device uses a similar periodic bias field of the form  $\mathbf{E}_B = E_0 \cos k_0 z \mathbf{e}_y$ , with the gas replaced by a semiconductor wafer and the radiation confined by a conducting wall, as shown in Fig. 1. The generation of photoinduced carriers, however, can be achieved with a much lower intensity ( $\sim 10^8$  W/cm<sup>2</sup>). The 1D analysis of a PPS is directly applicable to ionization of periodically biased gas. Included in this analysis are the effects of collisions.

The results of Sec. III describe the 1D limit of a PPS device. In the 1D limit, PPS radiation is generated with frequency  $\omega = c(\bar{k}_p^2 + k_0^2)/2k_0$ , wave number  $k_z = (\bar{k}_p^2 - k_0^2)/2k_0$ , and group velocity  $v_g = c(\bar{k}_p^2 - k_0^2)/(\bar{k}_p^2 + k_0^2)$ . Hence the wavelength of the radiation  $\lambda = 2\pi c/\omega$  can be tuned by adjusting the bias period  $\lambda_0 = 2\pi/k_0$  or the effective plasma wave number  $\bar{k}_p$  (i.e., via the carrier density  $n_n \propto \bar{k}_p^2$ ). In the absence of collisions,  $N_0$  periods of bias field generates  $N_0$  periods of radiation. For  $\bar{k}_p^2 \gg k_0^2$ , the electric field of the radiation is maximum and equal to the bias field  $E_0$ . The efficiency of converting the electrostatic field energy into radiation energy,  $\eta = W/W_0$ , is maximum when  $\bar{k}_p^2 = (5 + \sqrt{17})k_0^2/2$ , which implies  $\lambda \approx (0.6)^2\lambda_0$  and  $W/W_0 \approx 31\%$ . A finite collision frequency  $c\nu$  damps the radiation pulse and limits the pulse length  $L$  to a length shorter than the damping length  $L_d$ ,  $L \leq L_d$ , where  $L_d \propto \nu^{-1}$ .

The 2D theory of a PPS device is presented in Sec. IV. Analytic solutions describing the characteristics of the radiation pulse were obtained in the limit  $|\hat{k}_p^2 b^2| \ll 1$ . In 2D, radiation is generated in various modes characterized by the zeros of the dispersion relation, Eq. (30),  $s_n = ik_n - \gamma_n$ , where  $n$  is the mode number,  $\omega_n = ck_n$  is the mode frequency,  $v_g = c(k_n - k_0)/k_n$  is the axial group velocity, and  $\gamma_n \approx L_d^{-1}$  is the damping rate. In the limit  $|\hat{k}_p^2 b^2| \ll b/a \ll 1$ ,  $k_n$  and  $\gamma_n$  are given by Eqs. (32) and (33), respectively, and the power in the  $n$ th mode is given by Eq. (34). As  $k_p^2$  (proportional to the carrier density  $n_n$ ) increases, the mode frequency and power increase. In the limit  $b/a \ll |\hat{k}_p^2 b^2| \ll 1$ ,  $k_n$  and  $\gamma_n$  are

given by Eqs. (35) and (36), respectively, and the power in the  $n$ th mode is given by Eq. (37). Equation (38) implies that the energy conversion efficiency  $W_n/W_0$  is maximum when  $k_{x2}^2 = (5 + \sqrt{17})k_0^2/2$ , i.e., when  $a/l \approx 0.16\lambda_0$ . This corresponds to a wavelength  $\lambda_1 = 2\pi c/\omega_1 \approx 0.36\lambda_0$  and a maximum efficiency of  $W_n/W_0 \approx (6.3/l^2)\%$ .

To verify the analytic solutions, the full 2D dispersion relation Eq. (26) was solved numerically in Sec. V. In particular, the mode frequency  $ck_n$ , damping rate  $\gamma_n$ , and normalized power  $\hat{P}_n$ , Eq. (39), were plotted as a function of  $k_p$  (proportional to the square root of the carrier density  $n_n$ ) in Figs. 2(a), 2(b), and 4, respectively. For the parameters chosen (which are relevant to GaAs),  $a = 100\ \mu\text{m}$ ,  $b = 1\ \mu\text{m}$ ,  $L_y = 1\ \text{cm}$ ,  $E_0 = 10\ \text{kV/cm}$ ,  $\lambda_0 = 400\ \mu\text{m}$ , and  $1/\nu \approx 100\ \mu\text{m}$ , the normalized power for the fundamental ( $n=1$ ) was found to maximize at a value of  $k_p \approx 5 \times 10^3\ \text{cm}^{-1}$  (corresponding to a carrier density of  $n_n = 4.7 \times 10^{17}\ \text{cm}^{-3}$ ). This gave a radiation wavelength of  $\lambda_1 = 170\ \mu\text{m}$ , a damping length of  $\gamma_1^{-1} = 0.17\ \text{cm}$ , and a peak power of  $P_1 = 180\ \text{W}$ . The length of the radiation pulse is limited by collisions  $L \leq \nu_1^{-1}$ , which corresponds to a pulse duration  $L/c \leq 5.7\ \text{ps}$ . The length of radiation pulse can be controlled by adjusting the number of bias periods  $N_0$  and/or the damping rate  $\gamma_n$ . The wavelength of the radiation can be adjusted by adjusting the bias period  $\lambda_0$ , the carrier density, and/or the device dimensions.

This analysis indicates that a PPS device should be capable of generating peak radiation powers in the hundreds of watts and radiation wavelengths in the 50–500- $\mu\text{m}$  range. The pulse durations can be ultrashort,  $\leq 10\ \text{ps}$ , and, in principle, the device can provide control over the number of cycles of radiation generated. Such a source of radiation might have applications in the areas of far-infrared spectroscopy [6], the study of atomic (e.g., Rydberg) states [12], the characterization of materials (dielectrics, semiconductors, and superconductors) [13,14], and remote sensing.

#### ACKNOWLEDGMENTS

The authors acknowledge useful conversations with D. Papadopoulos, W. B. Mori, and T. Katsouleas, and the numerical assistance of J. Krall. This work was supported by the Office of Naval Research.

- 
- [1] G. Mourou, C. V. Stancampiano, and D. Blumenthal, *Appl. Phys. Lett.* **38**, 470 (1981).
- [2] D. H. Auston, K. P. Cheung, and P. R. Smith, *Appl. Phys. Lett.* **45**, 284 (1984).
- [3] B. B. Hu, J. T. Darrow, X. C. Zhang, and D. H. Auston, *Appl. Phys. Lett.* **56**, 886 (1990).
- [4] B. I. Greene, J. F. Federici, D. R. Dykaar, R. R. Jones, and P. H. Bucksbaum, *Appl. Phys. Lett.* **59**, 893 (1991).
- [5] N. M. Froberg, B. B. Hu, X. C. Zhang, and D. H. Auston, *IEEE J. Quantum Electron.* **28**, 2291 (1992).
- [6] B. I. Greene, P. N. Saeta, D. R. Dykaar, S. Schmitt-Rink, and S. L. Chuang, *IEEE J. Quantum Electron.* **QE-28**, 2303 (1992).
- [7] D. You, R. R. Jones, P. H. Bucksbaum, and D. R. Dykaar, *Opt. Lett.* **18**, 290 (1993).
- [8] R. R. Jones, D. You, and P. H. Bucksbaum, *Phys. Rev. Lett.* **70**, 1236 (1993).
- [9] A. S. Weling, B. B. Hu, N. M. Froberg, and D. H. Auston, *Appl. Phys. Lett.* **64**, 137 (1994).
- [10] D. You, R. R. Jones, P. H. Bucksbaum, and D. R. Dykaar, *J. Opt. Soc. Am. B* **11**, 486 (1994).
- [11] W. B. Mori, T. Katsouleas, J. M. Dawson, and C. H. Lai, *Phys. Rev. Lett.* **74**, 542 (1995).
- [12] R. R. Jones, N. E. Tielking, D. You, C. Raman, and P. H. Bucksbaum, *Phys. Rev. A* **51**, R2687 (1995).
- [13] D. Grischkowsky, S. Keiding, M. van Exter, and Ch. Fattinger, *J. Opt. Soc. Am. B* **7**, 2006 (1990).
- [14] M. C. Nuss, K. W. Goossen, J. P. Gordon, P. M. Mankiewich, and M. L. O'Malley, *J. Appl. Phys.* **70**, 2238 (1991).